Characterization of the parameter-mismatching effect on the loss of chaos synchronization

Alexey Jalnine[1] and Sang-Yoon Kim[2]
[1]*Department of Nonlinear Processes, Saratov State University, Astrkhanskaya St. 83, Saratov 410026, Russia*
[2]*Department of Physics, Kangwon National University, Chunchon, Kangwon-Do 200-701, Korea*
(Received 25 September 2001; published 18 January 2002)

We investigate the effect of the parameter mismatch on the loss of chaos synchronization in coupled one-dimensional maps. Loss of strong synchronization begins with a first transverse bifurcation of a periodic saddle embedded in the synchronous chaotic attractor (SCA), and then the SCA becomes weakly stable. Because of local transverse repulsion of the periodic repellers embedded in the weakly stable SCA, a typical trajectory may have segments of arbitrary length that have positive local transverse Lyapunov exponents. Consequently, the weakly stable SCA becomes sensitive with respect to the variation of the mismatching parameter. To quantitatively characterize such parameter sensitivity, we introduce a quantifier, called the parameter sensitivity exponent (PSE). As the local transverse repulsion of the periodic repellers strengthens, the value of the PSE increases. In terms of these PSEs, we also characterize the parameter-mismatching effect on the intermittent bursting and basin riddling occurring in the regime of weak synchronization.

DOI: 10.1103/PhysRevE.65.026210 PACS number(s): 05.45.Xt

I. INTRODUCTION

In recent years, synchronization in coupled chaotic systems has become a field of intensive study. For this case of chaos synchronization, a synchronous chaotic motion occurs on an invariant subspace of the whole phase space [1–4]. Particularly, this chaotic synchronization has attracted much attention, because of its potential practical application in secure communication [5].

In the ideal case a synchronous chaotic attracter (SCA) may exist on the invariant subspace. If such a SCA is stable against a perturbation transverse to the invariant subspace, it may become an attractor in the whole phase space. Such transverse stability of the SCA is intimately associated with transverse bifurcations of periodic saddles embedded in the SCA [6–12]. If all periodic saddles are transversely stable, the SCA becomes asymptotically stable (i.e., Lyapunov stable and attracting in a topological sense). For this case, we have ''strong'' synchronization. However, as the coupling parameter passes through a threshold value, a periodic saddle first becomes transversely unstable through a local bifurcation. After this first transverse bifurcation, a dense set of locally repelling ''tongues'' opens from the transversely unstable repeller and its preimages, and hence, trajectories falling into these tongues are locally repelled from the invariant subspace. Thus, loss of strong synchronization begins with such a first transverse bifurcation, and then we have ''weak'' synchronization. For this case, intermittent bursting or basin riddling may occur depending on the existence of an absorbing area, controlling the global dynamics, inside the basin of attraction [10–12]. In the presence of an absorbing area, acting as a bounded trapping vessel, locally repelled trajectories from the invariant subspace are restricted to move within the absorbing area, and exhibit transient intermittent bursting from the invariant subspace [13,14]. On the other hand, in the absence of such an absorbing area, the locally repelled trajectories will go to another attractor (or infinity), and hence the basin of attraction becomes riddled with a dense set of repelling tongues, belonging to the basin of another attractor (or infinity) [15].

However, in a real situation a small mismatch between the subsystems that destroys the invariant subspace is unavoidable. Hence, we investigate the effect of the parameter mismatching on the loss of synchronization in two coupled onedimenaional (1D) maps with an invariant diagonal. In the regime of weak synchronization, transversely unstable periodic repellers are embedded in the SCA. Hence, when a typical trajectory visits the repelling tongues that open from such repellers and their preimages, it experiences local transverse repulsion from the diagonal. As a result, the typical trajectory may have segments exhibiting positive local (finite time) transverse Lyapunov exponents, even if the averaged transverse Lyapunov exponent is negative. Because of the existence of these positive local transverse Lyapunov exponents, the weakly stable SCA becomes sensitive with respect to the variation of the mismatching parameter. This is in contrast to the case of the strong synchronization that has no such parameter sensitivity. Here we introduce a quantifier, called the parameter sensitivity exponent (PSE), that measures the ''degree'' of the parameter sensitivity in Sec. II. Hence, the PSE becomes a quantitative characteristic of the weakly stable SCA, as the phase sensitivity exponent quantitatively characterizes the degree of the strangeness of the strange nonchaotic attractors that appear typically in the quasiperiodically forced systems [16]. As the coupling parameter is varied away from the point of the first transverse bifurcation, successive transverse bifurcations of periodic saddles occur. Hence, the value of the PSE increases because local transverse repulsion of the periodic repellers embedded in the SCA becomes more and more strong, and it tends to infinity as c approaches the blow-out bifurcation point where the averaged transverse Lyapunov exponent becomes zero. As a result of this blow-out bifurcation, the weakly stable SCA becomes transversely unstable [17].

In terms of these PSEs, the effect of the parameter mismatching on the intermittent bursting and basin riddling is characterzied in Sec. III. For the case of bursting, any small

mismatching results in a continual sequence of intermittent bursts, called the attractor bubbling, where the long period of nearly synchronous state (laminar phase) is randomly interrupted by the short-time burst (burst phase). On the other hand, for the case of riddling, the SCA on the diagonal is transformed into a chaotic transient. In both cases, the quantity of interest is the average time that a trajectory spends near the diagonal (i.e., the average interburst interval and the average lifetime of the chaotic transient) [14]. As the PSE increases, local transverse repulsion of the periodic repellers embedded in the SCA becomes strong, and hence the average time τ that a typical trajectory spends near the diagonal becomes short. Note that τ may be quantitatively characterized in terms of the PSEs. Finally, we give a summary in Sec. IV.

II. CHARACTERIZATION OF THE PARAMETER SENSITIVITY OF THE SCA

We investigate the parameter-mismatching effect on the weak synchronization in two coupled 1D maps [12]

$$T:\begin{cases} x_{n+1}=F(x_n,y_n)=f(x_n,a)+(1-\alpha)cg(x_n,y_n), \\ y_{n+1}=G(x_n,y_n)=f(y_n,b)+c\,g(y_n,x_n), \end{cases} \tag{1}$$

where x_n and y_n are state variables of the subsystems at a discrete time n, local dynamics in each subsystem with a control parameter $p(p=a,b)$ is governed by the 1D map $f(x,p)=1-px^2$, c is a coupling parameter between the two subsystems, and $g(x,y)$ is a coupling function of the form,

$$g(x,y)=y^2-x^2. \tag{2}$$

For $\alpha=0$, the coupling becomes symmetric, while for nonzero α $(0<\alpha\leqslant 1)$ it becomes asymmetric. The extreme case of asymmetric coupling with $\alpha=1$ corresponds to the unidirectional coupling. In such a way, α tunes the degree of asymmetry in the coupling.

For the case of identical 1D maps (i.e., $a=b$), there exists an invariant synchronization line, $y=x$, in the x-y phase space. However, in the presence of a mismatching between the two 1D maps, the diagonal is no longer invariant. To take into consideration such a mismatching effect, we introduce a small mismatching parameter ε in the coupled 1D maps of Eq. (1) such that

$$b=a-\varepsilon, \tag{3}$$

and consider an orbit $\{(x_n,y_n)\}$ starting from an initial point on the diagonal (i.e., $x_0=y_0$). As the strength of the local transverse repulsion from the diagonal increases, the SCA becomes more and more sensitive with respect to the variation of ε. Such parameter sensitivity of the SCA for $\varepsilon=0$ may be characterized by calculating the derivative of the transverse variable $u_n(=x_n-y_n)$, denoting the deviation from synchronization, with respect to ε,

$$\begin{aligned} \left.\frac{\partial u_{n+1}}{\partial\varepsilon}\right|_{\varepsilon=0} &= \left.\frac{\partial x_{n+1}}{\partial\varepsilon}\right|_{\varepsilon=0} - \left.\frac{\partial y_{n+1}}{\partial\varepsilon}\right|_{\varepsilon=0} \\ &= \left[\left.\frac{\partial F(x_n,y_n)}{\partial x_n}\right|_{\varepsilon=0} - \left.\frac{\partial G(x_n,y_n)}{\partial x_n}\right|_{\varepsilon=0}\right]\left.\frac{\partial x_n}{\partial\varepsilon}\right|_{\varepsilon=0} \\ &\quad + \left[\left.\frac{\partial F(x_n,y_n)}{\partial y_n}\right|_{\varepsilon=0} - \left.\frac{\partial G(x_n,y_n)}{\partial y_n}\right|_{\varepsilon=0}\right]\left.\frac{\partial y_n}{\partial\varepsilon}\right|_{\varepsilon=0} \\ &\quad - \left.\frac{\partial G(x_n,y_n,\varepsilon)}{\partial\varepsilon}\right|_{\varepsilon=0}. \end{aligned} \tag{4}$$

Using Eq. (1), we may obtain a recurrence relation

$$\begin{aligned} \left.\frac{\partial u_{n+1}}{\partial\varepsilon}\right|_{\varepsilon=0} &= [f_x(x_n^*,a)-(2-\alpha)ch(x_n^*)]\left.\frac{\partial u_n}{\partial\varepsilon}\right|_{\varepsilon=0} \\ &\quad + f_a(x_n^*,a), \end{aligned} \tag{5}$$

where f_x and f_a are the derivatives of f with respect to x and a, $\{(x_n^*,y_n^*)\}$ is the synchronous orbit with $x_n^*=y_n^*$ for $\varepsilon=0$, and $h(x)$ is a reduced coupling function defined by [18]

$$h(x)\equiv\left.\frac{\partial g(x,y)}{\partial y}\right|_{y=x}. \tag{6}$$

Hence, starting from an initial orbit point (x_0^*,y_0^*) on the diagonal, we may obtain derivatives at all points of the orbit

$$\left.\frac{\partial u_N}{\partial\varepsilon}\right|_{\varepsilon=0} = \sum_{k=1}^{N} R_{N-k}(x_k^*)f_a(x_{k-1}^*,a) + R_N(x_0^*)\left.\frac{\partial u_0}{\partial\varepsilon}\right|_{\varepsilon=0}, \tag{7}$$

where

$$R_M(x_m^*)=\prod_{i=0}^{M-1}[f_x(x_{m+i}^*,a)-(2-\alpha)c\,h(x_{m+i}^*)]. \tag{8}$$

One can easily show that the factor $R_M(x_m^*)$ is associated with a local (M-time) transverse Lyapunov exponent $\sigma_M^T(x_m^*)$ of the SCA that is averaged over M synchronous orbit points starting from x_m^* as follows:

$$\sigma_M^T(x_m^*)=\frac{1}{M}\ln|R_M(x_m^*)|. \tag{9}$$

Thus, $R_M(x_m^*)$ becomes a local (stability) multiplier that determines local sensitivity of the motion during a finite time M. As $M\to\infty$, σ_M^T approaches the usual transverse Lyapunov exponent σ_T that denotes the average exponential rate of divergence of an infinitesimal perturbation transverse to the SCA. Since $\partial u_0/\partial\varepsilon|_{\varepsilon=0}=0$, Eq. (7) reduces to

$$\left.\frac{\partial u_N}{\partial\varepsilon}\right|_{\varepsilon=0} = S_N(x_0^*)\equiv\sum_{k=1}^{N} R_{N-k}(x_k^*)f_a(x_{k-1}^*,a). \tag{10}$$

In the case of weak synchronization, there are transversely unstable periodic repellers embedded in the SCA. When a typical trajectory visits neighborhoods of such repellers and their preimages, it has segments experiencing local repulsion from the diagonal. Thus, the distribution of local transverse Lyapunov exponents σ_M^T for a large ensemble of trajectories and large M may have a positive tail. For the segments of a trajectory exhibiting a positive local Lyapunov exponent ($\sigma_M^T>0$), the local multipliers R_M [$=\pm\exp(\sigma_M^T M)$] can be arbitrarily large, and hence the partial sum S_N may be arbitrarily large. This implies unbounded growth of the derivatives $\partial u_N/\partial\varepsilon|_{\varepsilon=0}$ as N tends to infinity, and consequently the weakly stable SCA may have a parameter sensitivity.

As an example, we consider the SCA that exists in the interval of $c_{b,l}[\simeq -2.963]<c<c_{b,r}[\simeq -0.677]$ for $a=1.82$ in the unidirectionally coupled case of $\alpha=1$. When the coupling parameter c passes through $c_{b,l}$ or $c_{b,r}$, the SCA becomes transversely unstable through a blow-out bifurcation, and then a complete desynchronization occurs. In the regime of synchronization, a strongly stable SCA exists for $c_{t,l}[\simeq -2.789]<c<c_{t,r}[\simeq -0.850]$. For this case of strong synchronization, there is no parameter sensitivity, because all periodic saddles embedded in the SCA are transversely stable. Hence, in the presence of a small parameter mismatching ε the strongly stable SCA becomes slightly perturbed, as shown in Figs. 1(a) and 1(b). However, when the coupling parameter c passes $c_{t,r}$ and $c_{t,l}$, bubbling and riddling transitions occur through the first transverse bifurcations of periodic saddles, respectively. For this case, the weakly stable SCA has a parameter sensitivity, because of local transverse repulsion of the periodic repellers embedded in the SCA. Thus, however small the parameter mismatching ε, a persistent intermittent bursting, called the attractor bubbling, occurs in the regime of bubbling ($c_{t,r}<c<c_{b,r}$), as shown in Figs. 1(c) and 1(d). On the other hand, in the regime of riddling ($c_{b,l}<c<c_{t,l}$), the weakly SCA with a riddled basin for $\varepsilon=0$ is transformed into a chaotic transient with a finite lifetime in presence of a parameter mismatch [see Fig. 1(e)]. As c is varied away from $c_{t,l}$ or $c_{t,r}$, transversely unstable periodic repellers appear successively in the SCA through transverse bifurcations. Then the degree of the parameter sensitivity of the SCA increases, because of the increase in the strength of local transverse repulsion of the periodic repellers. To quantitatively characterize the parameter sensitivity of the SCA, we iterate Eqs. (1) and (5) starting from an initial orbit point (x_0^*, y_0^*) on the diagonal and $\partial u_0/\partial\varepsilon|_{\varepsilon=0}=0$, and then we obtain the partial sum $S_N(x_0^*)$ of Eq. (10). The quantity S_N becomes very intermittent, as shown in Fig. 2(a). However, looking only at the maximum

$$\gamma_N(x_0^*)=\max_{0\leq n\leq N}|S_n(x_0^*)|, \tag{11}$$

one can easily see the boundedness of S_N. Figure 2(b) shows the functions γ_N for both cases of strong and weak synchronization. For the case of strong synchronization with $c=-1.5$, γ_N grows up to the largest possible value of the derivative $|\partial u/\partial\varepsilon|$ along the SCA and remains constant for all subsequent iterations. Thus, γ_N saturates for large N and hence the strongly stable SCA has no parameter sensitivity. On the other hand, for the case of weak synchronization with $c=-0.7$, γ_N grows unboundedly and exhibits no saturation. Consequently, the weakly stable SCA has a parameter sensitivity.

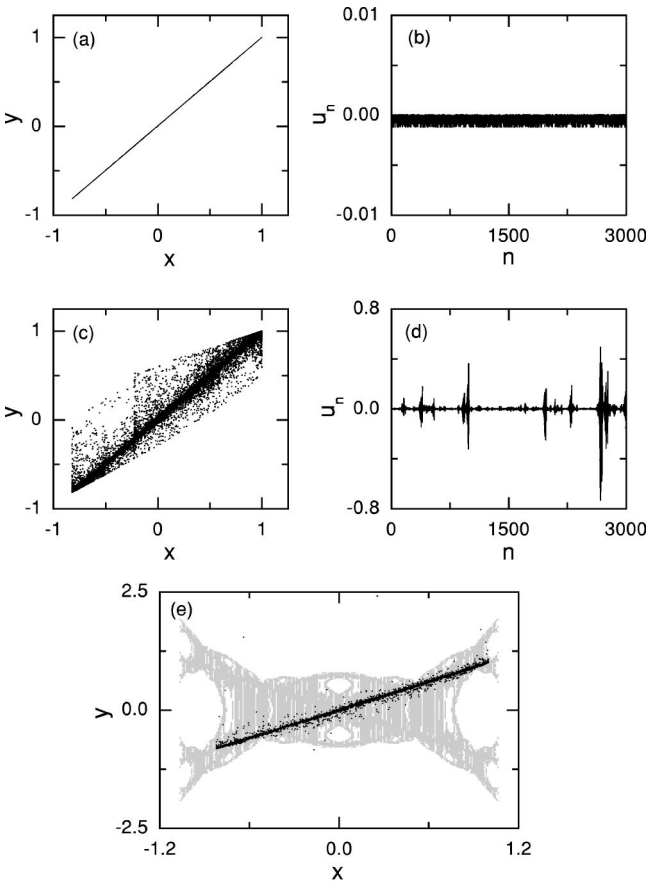

FIG. 1. Effect of the parameter mismatch with $\varepsilon=0.001$ on the chaos synchronization for $a=1.82$ in the unidirectionally coupled case of $\alpha=1$. (a) A slightly perturbed SCA and (b) the evolution of the transverse variable $u_n(x_n-y_n)$ vs the discrete time n for the case of strong synchronization with $c=-1.5$. (c) A bubbling attractor and (d) the evolution of u_n vs n for the bubbling case of $c=-0.7$. For the riddling case of $c=-2.91$ the SCA with a basin (gray region) riddled with a dense set of tongues leading to divergent orbits (white region) for $\varepsilon=0$ is transformed into a chaotic transient (black dots) for $\varepsilon=0.001$ as shown in (e).

The growth rate of the function $\gamma_N(x_0^*)$ with time N represents a degree of the parameter sensitivity, and can be used as a quantitative characteristic of the weakly stable SCA. However, $\gamma_N(x_0^*)$ depends on a particular trajectory. To obtain a representative quantity, we consider an ensemble of randomly chosen initial points (x_0^*, y_0^*) on the diagonal, and take the minimum value of γ_N with respect to the initial orbit points

$$\Gamma_N=\min_{x_0^*}\gamma_N(x_0^*). \tag{12}$$

Figure 3 shows a parameter sensitivity function Γ_N for $c=-0.7$. Note that Γ_N grows unboundedly with some power

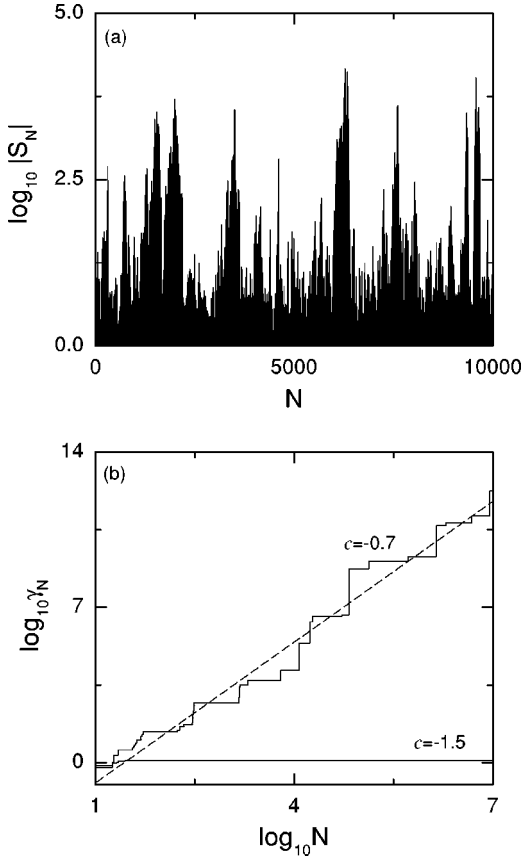

FIG. 2. (a) Intermittent behavior of the partial sum $|S_N|$ for $\alpha=1$, $a=1.82$, and $c=-0.7$. (b) Two functions γ_N looking only at the maximum for $c=-1.5$ (strong synchronization) and $c=-0.7$ (weak synchronization). These results are obtained for the trajectory starting from the initial orbit point $(x_0^*, y_0^*)=(0.5,0.5)$ in the case of $\alpha=1$ and $a=1.82$.

$$\Gamma_N \simeq N^{\delta}. \tag{13}$$

Here the value $\delta \simeq 2.58$ is a quantitative characteristic of the parameter sensitivity of the SCA, and we call it the PSE. In each regime of bubbling or riddling, we vary the coupling parameter from the bubbling or riddling transition point to the blow-out bifurcation point and obtain the PSEs. For obtaining satisfactory statistics, we consider 100 ensembles for each c, each of which contains 100 randomly chosen initial orbit points and choose the average value of the 100 PSEs obtained in the 100 ensembles. Figure 4(a) shows the plot of such PSEs versus c. Note that the PSE δ monotonically increases as c is varied away from the bubbling or riddling transition point, and tends to infinity as c approaches the blow-out bifurcation point. This increase in the parameter sensitivity of the SCA is caused by the increase in the strength of local transverse repulsion of the periodic repellers embedded in the SCA. After the blow-out bifurcation, the weakly stable SCA is transformed into a transversely unstable chaotic saddle exhibiting an exponential parameter sensitivity as shown in Fig. 4(b). Thus, a complete desynchronization occurs.

We also discuss the distribution of positive local (M-time) transverse Lyapunov exponents, causing the parameter sensitivity of the weakly stable SCA. As an example, we consider the case of $a=1.82$ and $c=-0.7$ and obtain the probability distribution $P_M(\sigma)$ of local (M-time) transverse Lyapunov exponents, where $P_M(\sigma)d\sigma$ is the probability that σ_M^T has a value between σ and $\sigma+d\sigma$, by taking a long trajectory dividing it into segments of length M and calculating σ_M^T in each segment. Figure 5(a) shows the distributions $P_M(\sigma)$ for $M=100$, 500, and 900. In the limit $M\to\infty$, $P_M(\sigma)$ approaches the delta distribution $\delta(\sigma-\sigma_T)$, where σ_T is the usual averaged transverse Lyapunov exponent. However, for finite M there is a variance $\langle(\sigma_M^T-\langle\sigma_M^T\rangle)^2\rangle$ $[\equiv\int_{-\infty}^{\infty}P_M(\sigma)(\sigma-\langle\sigma_M^T\rangle)^2d\sigma]$ from the average value $\langle\sigma_M^T\rangle$ $[\equiv\int_{-\infty}^{\infty}P_M(\sigma)\sigma d\sigma]$. As shown in Fig. 5(b) this variance approaches zero inversely with M as follows:

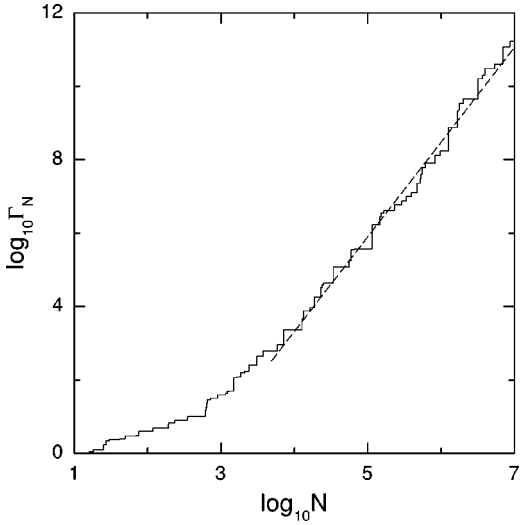

FIG. 3. Parameter sensitivity function Γ_N for $\alpha=1$, $a=1.82$, and $c=-0.7$ that takes the minimum value of γ_N in the ensemble containing 100 randomly chosen initial orbit points on the diagonal.

$$\langle(\sigma_M^T-\langle\sigma_M^T\rangle)^2\rangle=\frac{2D}{M}. \tag{14}$$

Here the value of $D(\simeq 0.054)$ is the same, independently of the values of c for $a=1.82$ in the regime of weak synchronization. One remarkable feature of the distribution is the slow decay of the positive tail of the distribution. In order to quantify this, we define the fraction of positive local Lyapunov exponents as

$$F_M^+=\int_0^{\infty}P_M(\sigma)d\sigma. \tag{15}$$

These fractions F_M^+'s are plotted for $c=-0.7$, -0.695, and -0.69 in Fig. 5(c). Note that for each value of c, the fraction F_M^+ exhibits a power-law decay,

$$F_M^+\sim M^{-\eta}. \tag{16}$$

Here the values of the exponent η decreases as c increases. Consequently, for any case of weak synchronization a trajectory has segments of arbitrarily long M that have positive

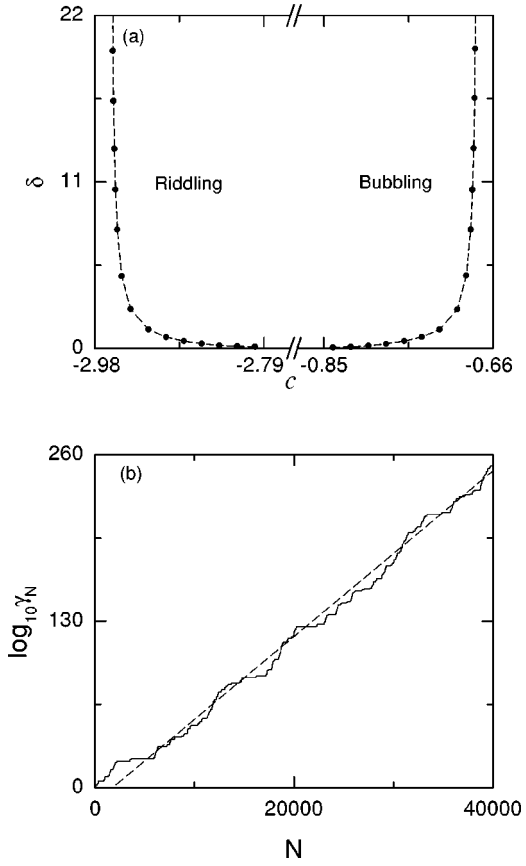

FIG. 4. (a) The plot of the PSEs δ vs c in the regime of weak synchronization for $\alpha=1$ and $a=1.82$. (b) The exponential parameter sensitivity for the trajectory starting from the initial point (0.5,0.5) for $\alpha=1$, $a=1.82$, and $c=-0.66$.

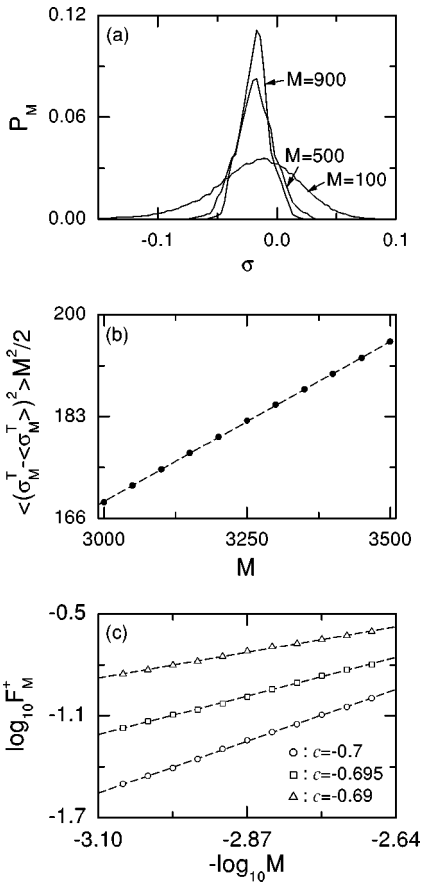

FIG. 5. (a) Three probability distributions P_M of the local M-time Lyapunov exponents for $M=100$, 500, and 900 when $\alpha=1$, $a=1.82$, and $c=-0.7$. (b) The plot of $\langle(\sigma_M^T-\langle\sigma_M^T\rangle)^2\rangle M^2/2$ vs M when $\alpha=1$, $a=1.82$, and $c=-0.7$. Note that the variance decreases inversely with M. (c) Plots of $\log_{10}F_M^+$(F_M^+: fraction of the positive local transverse Lyapunov exponent) vs $-\log_{10}M$. Note that the three plots for $c=-0.7$ (circles), -0.695 (squares), and -0.69 (triangles) are well fitted with the straight lines with the slopes $\eta=1.33$, 0.99, and 0.66, respectively. Hence, F_M^+ decays with some power η.

local Lyapunov exponents, and then the partial sum S_N in Eq. (10) may be arbitrarily large. Thus, the weakly stable SCA may have a parameter sensitivity. As shown in Fig. 5(c), as c increases the value of F_M^+ becomes larger. Hence, the degree of the parameter sensitivity of the weakly stable SCA increases.

So far, we have characterized the parameter mismatching effect in terms of the PSEs in the unidirectionally coupled case with the asymmetry parameter $\alpha=1$. Through Eq. (5), one can easily see that the PSE for a given (a,c) in the case of $\alpha=1$ is the same as that for the value of $[a,c/(2-\alpha)]$ in other coupled 1D maps with $0\leqslant\alpha<1$ in Eq. (1). Thus, the results of the PSEs given in Fig. 4(a) may be converted into those for the case of general α only by a scale change in the coupling parameter such that $c\rightarrow c/(2-\alpha)$. For this case, the bubbling regime for the case of $\alpha=1$ is always transformed into a bubbling regime for any other value of α, because the bubbling transition occurs through the first transverse supercritical period-doubling bifurcation, independently of the value of α. However, the riddling regime for the case of $\alpha=1$ is transformed into a bubbling or riddling regime depending on the value of α. For example, for the symmetrically coupled case of $\alpha=0$, the riddling regime for $\alpha=1$ is transformed into a bubbling regime, because a bubbling transition occurs through a first trasnverse supercritical pitchfork bifurcation. For all other asymmetric cases with nonzero α, the transtion to the weak synchronization occurs through the first transverse transcritical bifurcation. Depending on whether or not such a transcritical bifurcation induces a contact between the saddle fixed-point embedded in the SCA and the repelling fixed point on the basin boundary, a riddling or bubbling transtion occurs. Thus, a bubbling transition occurs through a transcritical noncontact bifurcation for small α, while a riddling transition takes place through a transcritical contact bifurcation for the values close to $\alpha=1$. For more details, refer to Ref. [12].

III. CHARACTERIZATION OF THE BUBBLING ATTRACTOR AND THE CHAOTIC TRANSIENT

We characterize the parameter-mismatching effect on the bubbling and riddling in terms of the PSEs for $a=1.82$ in the unidirectionally coupled case of $\alpha=1$. The quantity of interest in both cases is the average time τ that a typical trajectory

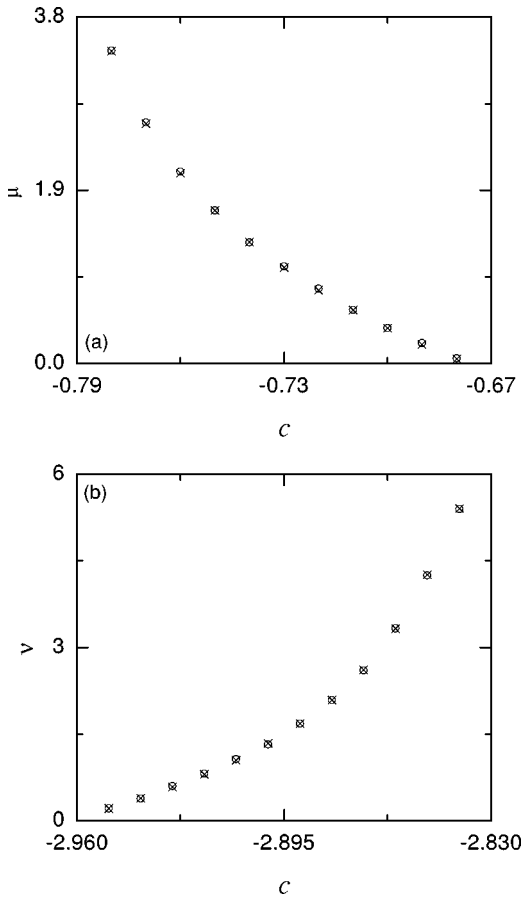

FIG. 6. (a) The plot of the laminar phase exponents (LPEs) μ (open circles) vs c for $\alpha=1$ and $a=1.82$. They agree well with the reciprocals of the PSEs (crosses). (b) The plot of the chaotic transient exponents (CTEs) (open circles) vs c for $\alpha=1$ and $a=1.82$. They agree well with the reciprocals of the PSEs (crosses).

spends near the diagonal. As c is varied from the bubbling or riddling transition point, such average time becomes short because the strength of local transverse repulsion of the periodic repellers embedded in the SCA increases. For the case of bubbling, the bubbling attractor is in the laminar phase when the magnitude of the deviation from the diagonal is less than a threshold value u_b^* (i.e., $|u_n|<u_b^*$). Otherwise, it is in the bursting phase. Here u_b^* is very small compared to the maximum bursting amplitude and it is the maximum deviation from the diagonal that may be acceptable in the context of synchronization. For each c, we follow the trajectory starting from the initial condition (0,0) until 50 000 laminar phases are obtained, and then we get the average laminar length τ (i.e., the average interburst interval) that scales with ε as [19]

$$\tau \sim \varepsilon^{-\mu}, \tag{17}$$

where μ will be referred to the laminar phase exponent (LPE). The plot of the LPE μ versus c is shown in Fig. 6(a). As c increases, the value of μ decreases, because the average laminar length shortens. Note that this LPE μ is associated with the PSE δ as follows. For a given ε, consider a trajectory starting from a randomly chosen initial orbit point on the diagonal. Then, From Eq. (13) the ''average'' time τ at which the magnitude of the deviation from the diagonal becomes the threshold value u_b^* can be obtained

$$\tau \sim \varepsilon^{-1/\delta}. \tag{18}$$

Thus, the two exponents have a reciprocal relation

$$\mu = 1/\delta. \tag{19}$$

The reciprocal values of δ are also plotted in Fig. 6(a), and they agree well with the values of μ. This reciprocal relation is valid also in the riddling regime. For each c we consider an ensemble of trajectories starting from 1000 randomly chosen initial points on the diagonal, and obtain the average lifetime of the chaotic transients. A trajectory may be regarded as having escaped once the magnitude of deviation u_n from the diagonal becomes larger than a threshold value u_c^* such that an orbit point with $|u|>u_c^*$ lies sufficiently outside the basin of the SCA. Thus, the average lifetime τ_c is found to scale with ε as [19]

$$\tau_c \sim \varepsilon^{-\nu}, \tag{20}$$

where ν will be referred to the chaotic transient exponent (CTE). The plot of the CTE ν versus c is given in Fig. 6(b). Like the bubbling case, the PSE and CTE also have a reciprocal relation (i.e., $\nu=1/\delta$), as shown in Fig. 6(b).

IV. SUMMARY

We have introduced a quantifier, called the PSE, to quantitatively characterize the sensitivity of the SCA with respect to the variation of the mismatching parameter in coupled 1D maps. Due to the existence of positive local Lyapunov exponents, the weakly stable SCA exhibits a parameter sensitivity, in contrast to the case of strongly stable SCA without such parameter sensitivity. In terms of these PSEs, we have also characterized the average laminar length and the average lifetime of the chaotic transient. Finally, we expect that the method of characterizing the parameter sensitivity of the SCA in terms of the PSEs may be generalized to the coupled systems consisting of the high-dimensional maps such as the Hénon map or the oscillators.

ACKNOWLEDGMENTS

S.Y.K. thanks W. Lim for his assistance in the numerical computations and A. J. thanks Professor S. P. Kuznetsov for fruitful discussions. This work was supported by the Interdisciplinary Research Program of the Korea Science and Engineering Foundation under Grant No. R01-1999-00021 and by the CRDF Grant No. REC-006.

[1] H. Fujisaka and T. Yamada, Prog. Theor. Phys. **69**, 32 (1983).
[2] A. S. Pikovsky, Z. Phys. B: Condens. Matter **50**, 149 (1984).
[3] V. S. Afraimovich, N. N. Verichev, and M. I. Rabinovich, Radiophys. Quantum Electron. **29**, 795 (1986).
[4] L. M. Pecora and T. L. Carroll, Phys. Rev. Lett. **64**, 821 (1990).
[5] K. M. Cuomo and A. V. Oppenheim, Phys. Rev. Lett. **71**, 65 (1993); L. Kocarev, K. S. Halle, K. Eckert, L. O. Chua, and U. Parlitz, Int. J. Bifurcation Chaos Appl. Sci. Eng. **2**, 973 (1992); L. Kocarev and U. Parlitz, Phys. Rev. Lett. **74**, 5028 (1995); N. F. Rulkov, Chaos **6**, 262 (1996).
[6] P. Ashwin, J. Buescu, and I. Stewart, Nonlinearity **9**, 703 (1996).
[7] Y.-C. Lai, C. Grebogi, J. A. Yorke, and S. C. Venkataramani, Phys. Rev. Lett. **77**, 55 (1996).
[8] V. Astakhov, A. Shabunin, T. Kapitaniak, and V. Anishchenko, Phys. Rev. Lett. **79**, 1014 (1997).
[9] Yu. L. Maistrenko, V. L. Maistrenko, A. Popovich, and E. Mosekilde, Phys. Rev. E **57**, 2713 (1998); **60**, 2817 (1999); O. Popovych, Yu. L. Maistrenko, E. Moskilde, A. Pikovsky, and J. Kurths, Phys. Lett. A **275**, 401 (2000); Phys. Rev. E **63**, 036 201 (2001).
[10] Yu. L. Maistrenko, V. L. Maistrenko, A. Popovich, and E. Mosekilde, Phys. Rev. Lett. **80**, 1638 (1998); G.-I. Bischi and L. Gardini, Phys. Rev. E **58**, 5710 (1998).
[11] S.-Y. Kim and W. Lim, Phys. Rev. E **63**, 026 217 (2001); S.-Y. Kim, W. Lim, and Y. Kim, Prog. Theor. Phys. **105**, 187 (2001).
[12] S.-Y. Kim and W. Lim, Phys. Rev. E **64**, 016 211 (2001).
[13] P. Ashwin, J. Buescu, and I. Stewart, Phys. Lett. A **193**, 126 (1994); J. F. Heagy, T. L. Carroll, and L. M. Pecora, Phys. Rev. E **52**, 1253 (1995); S. C. Venkataramani, B. R. Hunt, E. Ott, D. J. Gauthier, and J. C. Bienfang, Phys. Rev. Lett. **77**, 5361 (1996).
[14] S. C. Venkataramani, B. R. Hunt, and E. Ott, Phys. Rev. E **54**, 1346 (1996).
[15] J. C. Alexander, J. A. Yorke, Z. You, and I. Kan, Int. J. Bifurcation Chaos Appl. Sci. Eng. **2**, 795 (1992); E. Ott, J. C. Sommerer, J. C. Alexander, I. Kan, and J. A. Yorke, Phys. Rev. Lett. **71**, 4134 (1993); J. C. Sommerer and E. Ott, Nature (London) **365**, 136 (1993); E. Ott, J. C. Alexander, I. Kan, J. C. Sommerer, and J. A. Yorke, Physica D **76**, 384 (1994); J. F. Heagy, T. L. Carroll, and L. M. Pecora, Phys. Rev. Lett. **73**, 3528 (1994).
[16] A. Pikovsky and U. Feudel, Chaos **5**, 253 (1995).
[17] E. Ott and J. C. Sommerer, Phys. Lett. A **188**, 39 (1994); Y. Nagai and Y.-C. Lai, Phys. Rev. E **56**, 4031 (1997).
[18] S.-Y. Kim and H. Kook, Phys. Rev. A **46**, R4467 (1992).
[19] S.-Y. Kim, W. Lim, and Y. Kim, Prog. Theor. Phys. (to be published).